



## Effects of high hydrostatic pressure on physicochemical and functional properties of soybean protein isolate

Fei ZHAO<sup>1,2#\*</sup> , Xuemei LIU<sup>3#</sup>, Meng LIAN<sup>4</sup>, Yongqi YANG<sup>4</sup>, Chunlei LI<sup>2</sup>, Haicheng XU<sup>2</sup>, Wenchao CAO<sup>2</sup>, Limin ZHENG<sup>1,2</sup>, Haizhou DONG<sup>5</sup>, Wentao WANG<sup>5\*</sup>

### Abstract

Impacts of high hydrostatic pressure (HHP) pretreatment on the physicochemical, functional and antioxidant properties of soybean protein isolate (SPI) were investigated. Changes in the secondary and tertiary structures were determined by Fourier transform infrared spectra and fluorescence spectra. The particle sizes reduced from 217.20 nm to 192.70 nm while the zeta potential increased. It's revealed by scanning electron microscopy that the HHP treatment could result in the formation of large aggregation, leaving the SPI with irregular and uneven surface. Moreover, hollow spheres were also observed in SPI by means of dynamic and static light scattering. As a result, the foaming capacity of HHP-treated SPI and antioxidant activity of the HHP-treated SPI hydrolysates were improved significantly.

**Keywords:** high hydrostatic pressure; soybean protein isolates; structure;  $\zeta$ -potential; dynamic and static light scattering; functional properties.

**Practical Application:** The conformational characterization and aggregation of HHP-treated SPI were investigated, which has not been studied at present. The foaming capacity of HHP-treated SPI and antioxidant activity of the HHP-treated SPI hydrolysates increased significantly. The results help facilitate the development of high technology in the protein industry.

### 1 Introduction

Soybean protein isolate is one of the most important commercial plant protein and may be the cheapest source of protein with high nutritional value. SPI contains about 90% protein and is used as an ingredient in bread products, beverages and meat products (Torrezan et al., 2007; Nogueira et al., 2022). Proteins present versatility during processing and improve dynamic functional properties of foods (e.g., solubility and hydrodynamic properties). The surface activity, foaming and emulsification properties of a protein can exert significant influences on its solubility. The tertiary and quaternary structures of protein is compact, which bring about poor functional performance of protein (Yuan et al., 2012). The functional characteristics can be influenced by various factors: pH, ionic strength and chemical, physical, enzymatic modifications, etc. The combination of multiple modification methods could improve the functional characteristics of proteins (Jia et al., 2010; Wang et al., 2016; Furtado et al., 2017).

High hydrostatic pressure is a non-thermal processing technology that has been used for the modification of protein. HHP was applied to preserve the native properties of food in milk or colostrum, and could denature native milk proteins leading to altered immunogenicity (Huppertz et al., 2004; Indyk et al., 2008; Bogahawaththa et al., 2018). HHP treatment has been demonstrated

to influence the functional properties of proteins through the disruption and reformation of hydrophobic interactions and hydrogen bonds leading to denaturation, gelation and aggregation (Cheftel, 1992; López-Fandiño, 2006; Ahmed et al., 2008). Tang & Ma (2009) observed that HHP treatment (200-600 MPa) led to formation of SPI aggregates and resulted in gradual unfolding of proteins rebuilding their secondary and tertiary structures after pressure releasing. HHP-treatment of whey protein isolates and kidney bean protein isolate influenced denaturation of protein resulting change in emulsifying and foaming properties (Krešić et al., 2006; Ahmed et al., 2018). Shao et al. (2018) found that the meat yield and shucking of red swamp crayfish increased and the moisture content decreased after the high pressure treatments. HHP treatment could significantly reduce the allergenicity of ginkgo seed protein and enhance dairy whey protein hydrolysis to obtain peptides of hypoallergenic infant formulae (Peñas et al., 2006).

The aim of our study was to assess the effects of HHP treatments to assist the enzymatic hydrolysis of SPI, in order to increase their antioxidant activities. Moreover, the influence of high pressure on some physicochemical and functional properties of protein was well documented, including structure, particle size,  $\zeta$ -potential, foaming properties of SPI and the

Received 01 Sept., 2022

Accepted 23 Oct., 2022

<sup>1</sup>Department of Food Quality and Safety, Jia-Sixie College of Agriculture, Weifang University of Science and Technology, Wei'fang, Shandong, China

<sup>2</sup>Shandong Facility Horticulture Bioengineering Research Center, Weifang University of Science and Technology, Wei'fang, China

<sup>3</sup>Jinan Fruit Research Institute, All-China Federation of Supply and Marketing Co-operatives, Ji'nan, Shandong, China

<sup>4</sup>College of Chemical Engineering and Environment, Weifang University of Science and Technology, Wei'fang, Shandong, China

<sup>5</sup>Department of Food Science and Engineering, Shandong Agricultural University, Tai'an, Shandong, China

\*Corresponding author: feizhaozhaofei@126.com; wangwt@sdau.edu.cn

<sup>#</sup>These authors are equal to this work

antioxidant activity of SPI hydrolysates. The conformational characterization and aggregation of HHP-treated SPI were investigated. The results help facilitate the development of high technology in the protein industry.

## 2 Materials and methods

### 2.1 Materials

Soybean protein isolate (SPI; protein content 90.31%) was provided by Shandong Wonderful Industrial Group Co. Ltd. (Shandong Province, China). Bromelain was supplied by Guangxi Pangbo biological engineering Co. Ltd. (Guangxi Province, China).

### 2.2 High hydrostatic pressure treatment of SPI

SPI powder (5.0 g) was dissolved in deionized water (100 mL) under stirring for 2 h and stored at 4 °C overnight. The HHP pretreatment was carried out in a high-pressure machine (HPP600MPA/3-5L, Baotou Kefa High Pressure Technology Co. Ltd., Baotou, China) with a pressure vessel. The capacity of reactor tank was 3 L (300 mm in height and 100 mm in diameter), and a water jacket was used as temperature control. SPI solutions were vacuum sealed in a polyethylene bag. The SPI solutions (5.0 g/100 mL) were subjected to HHP treatment at 100, 200, 300, 400 and 500 MPa. The target pressure was achieved within 1-2 min, held for 5, 15 and 30 min, and released to atmospheric pressure within 1-2 min. Samples were freeze-dried for further use. The untreated sample was used as the control.

### 2.3 Fourier transformed infrared spectroscopy

An FTIR spectrometer (Nicolet iS5, Thermo SCIENTIFIC) was used to analyze the SPI samples. Samples were prepared as pellets using potassium bromide, which were scanned 32 times at 4 cm<sup>-1</sup> resolution from 4000 to 500 cm<sup>-1</sup>. The spectra of the samples were analyzed using the Omnic software (OMNIC 8.2) (Wang et al., 2011a).

### 2.4 Fluorescence measurements

The fluorescence of SPI samples (0.2 mg/mL) were measured with fluorescence spectrometer (Lumina, Thermo Fisher, America) at 290 nm excitation wavelength (slit = 5 nm) and 300-500 nm emission wavelength (slit = 5 nm). The sample solutions were prepared in 10 mM phosphate buffer (pH 7.0) (Zhao et al., 2019; Wang et al., 2022).

### 2.5 Particle size determination

The particle size of the HHP treated SPI samples were measured by NanoBrook ZetaPlus Potential Analyzer (Brookhaven Instruments, Holtsville, NY, USA). The effective diameter of samples was calculated from the instrument software for three time.

### 2.6 Zeta ( $\zeta$ ) potential measurements

The  $\zeta$ -potentials of the samples were performed by Zeta potential analyzer (ZetaPlus, Brookhaven Instruments, Holtsville,

NY, USA). The sample solutions filtered through 0.45  $\mu$ m Millipore filters and transferred into the cuvette for 30 min before measurements. The zeta potential value was the average of three measurements.

### 2.7 Scanning Electron Microscopy (SEM)

The microstructure of the HHP-treated SPI was examined through a SEM (ZEISS, Jena, Germany). The samples were photographed at different magnifications (200  $\times$  and 2000  $\times$ ).

### 2.8 Light scattering

Dynamic and static light scattering were conducted using BI-200SM dynamic laser scattering system (Brookhaven Instruments, Holtsville, NY, USA). The light source was a 35 mW helium neon laser (wave length of 633 nm). The sample solutions prepared for light scattering measurements were filtered with 0.45  $\mu$ m Millipore filters and placed into precision cylindrical cell (quartz, diameter: 25 mm). Static light scattering measurements were measured in the angular range of 30-120° and dynamic measurements were carried out in the angular range of 30-90°. The refractive index increment ( $dn/dc$ ) was measured as 0.185 mL/g for SPI aqueous solution (Zhao et al., 2018). The autocorrelation functions were used CONTIN and NNLS methods for analysis. All the light scattering measurements were determined at 25 ± 0.01 °C by a water-recycling system.

### 2.9 Foaming ability and foaming stability

SPI dispersions (4%, w/v, 40 mL) after HHP treatment were blended with a rotor-stator disperser (T18 digital Ultra-T, IKA) at 8000 rpm for 1 min. After blending, the foam was decanted into a 100 mL graduated cylinder rapidly. Foaming ability (FA) was measured by comparing the foam volume (2 min) to the initial sample liquid volume. Foam stability (FS) was determined by comparing the foam volume at 10, 20 and 30 min to the initial sample foam volume (Puteri et al., 2018; Xiong et al., 2018) (Equations 1-2).

$$FA(\%) = V_0 / 40 \times 100 \quad (1)$$

$$FS(\%) = V_t / V_0 \times 100 \quad (2)$$

Where  $V_0$  is the foam volume at 2 min,  $V_t$  is the foam volume at 10, 20 and 30 min.

### 2.10 Preparation of SPI hydrolysates

In the enzymatic hydrolysis experiments, the pH of untreated and HHP-treated sample solutions (5% w/v, 50 mL) were adjusted to 7.0 with NaOH, then the enzymatic solution was added (1:10 (w/w)) to protein solution. Samples were hydrolyzed at the optimal temperature (55 °C for bromelain) for 3 h. The enzymatic reactions was stopped by heating the samples at 100 °C for 10 min, subsequently with a rapid cooling in an ice bath. The enzymatic hydrolysates of samples were centrifuged at 10,000 g for 10 min, and the supernatant was freeze-dried for further analysis.

## 2.11 Degree of hydrolysis

The degree of hydrolysis (DH) was measured by the pH-stat method according to the method of our previous works (Zhao et al., 2018). The DH was calculated by the Equation 3:

$$DH = \frac{B \times N}{\alpha \times M_p \times h} \times 100\% \quad (3)$$

Where B is consumption of the NaOH (mL), N is the NaOH concentration (1 M),  $\alpha$  is the degree of  $\alpha$ -amino groups dissociation,  $M_p$  is the protein mass (g), and for SPI,  $h = 7.75$  mmol/g protein.

## 2.12 Determination of antioxidant activity of SPI hydrolysates

The antioxidant activity of SPI hydrolysates was evaluated by 1,1-diphenyl-2-picrylhydrazyl (DPPH), and the DPPH radical-scavenging activity of the hydrolysates was measured with the method of Zhao et al. (2018). An aliquot (2 mL) of the sample hydrolysate solution (5.0 mg/mL) was added to 2 mL of 20  $\mu$ M ethanolic DPPH solution. The mixture was incubated for 30 min at 30 °C. The absorbance was determined at 517 nm with a spectrophotometer. The antioxidant activity of the SPI hydrolysates was evaluated based on the Equation 4:

$$DPPH \text{ scavenging activity } (\%) = (1 - \frac{A_i - A_j}{A_0}) \times 100\% \quad (4)$$

Where  $A_i$  is the absorbance of the SPI hydrolysate with DPPH,  $A_j$  is the absorbance of the SPI hydrolysate with ethanol, and  $A_0$  is the absorbance of distilled water with DPPH.

## 2.13 Data analysis

Data were presented as the means  $\pm$  standard deviations (SD) of three replicate determinations. Analysis of Fourier transform infrared spectroscopy and fluorescence spectroscopy was conducted using OMNIC software (Thermo Fisher Scientific, Waltham, MA, USA) and PeakFit software version 4.0 (Systat Software Inc, San Jose, California, USA).

## 3 Results and discussion

### 3.1 Fourier transform infrared spectroscopy analysis

FTIR spectra of untreated and HHP treated SPI were described the secondary structure changes in Figure 1. The main bands included amide I ( $1700$ - $1600$  cm $^{-1}$ , C=O stretching) amide II ( $1530$  cm $^{-1}$ , N-H bending and C-H stretching vibrations) and amide III ( $1236$  cm $^{-1}$ , C-N stretching and N-H bending vibrations). From the Figure 1, HHP treatment induced marked changes in the intensity and wavenumber of the SPI absorption peaks. The amide I (about  $3$  cm $^{-1}$ ), amide II (about  $7$  cm $^{-1}$ ) and III (about  $1$  cm $^{-1}$ ) band peaks of SPI generated blue shift after HHP treatment, while the amide A (N-H stretching vibrations) band peaks of SPI generated red shift (about  $5$  cm $^{-1}$ ). The HHP treatment also induced a significant blue shift (about  $17$ - $50$  cm $^{-1}$ ) of the C=S stretching vibration ( $1153$  cm $^{-1}$ ) band peaks of SPI, with increasing of absorption intensity. The result indicated that hydrogen bonds were formed within the molecules, and the bonding constant of N-H bond decreased. The amide B band peaks (N-H stretching vibrations) of SPI showed red shift (about  $2$  cm $^{-1}$ ) after HHP treatment at  $100$ - $300$  MPa, while blue shift (about  $2$  cm $^{-1}$ )  $400$ - $500$  MPa. Ahmed et al. (2018) found that

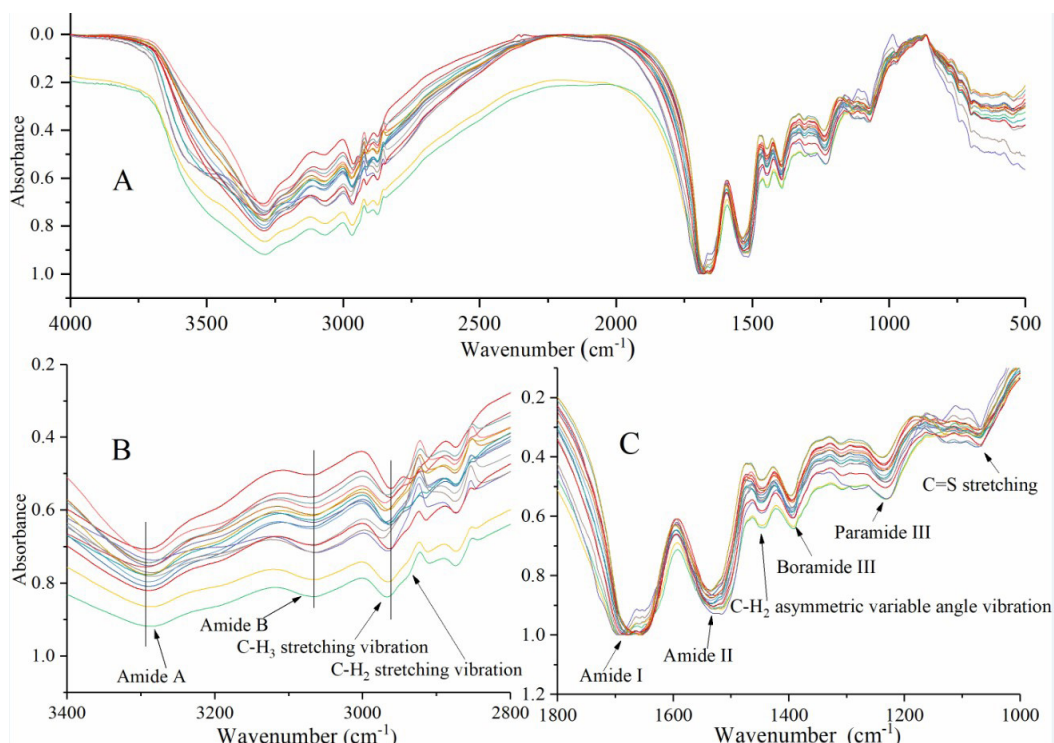


**Figure 1.** FTIR spectra of SPI after HHP treatment (A: 4,000-500 cm $^{-1}$ , B: 3,400-2,800 cm $^{-1}$ , C: 1,800-1,000 cm $^{-1}$ ).

HHP treatment induced shift in the wavelength of kidney bean protein isolate (amide I and amide II). The results showed that HHP treatment could change the secondary structure of SPI, which due to the interactions between the protein molecules were destroyed by pressure treatment.

The spectra in amide I band ( $1700\text{-}1600\text{ cm}^{-1}$ ) were used for deconvolution and curve fitting. The secondary structural information can be got from the deconvoluted spectra analysis. The amide I band includes  $\alpha$ -helix ( $1650\text{-}1658\text{ cm}^{-1}$ ),  $\beta$ -sheet ( $1640\text{-}1610\text{ cm}^{-1}$  and  $1680\text{-}1690\text{ cm}^{-1}$ ),  $\beta$ -turn ( $1670\text{-}1660\text{ cm}^{-1}$  and  $1690\text{-}1700\text{ cm}^{-1}$ ), and random coil ( $1640\text{-}1650\text{ cm}^{-1}$ ). The effects of pressure and time on the secondary structure were displayed in Figure 2. Compared with the native SPI, the  $\alpha$ -helix and  $\beta$ -turn contents of HHP-treated samples (100-400 MPa) increased, while that of the  $\beta$ -sheet and random coil decreased. The results indicated that the  $\beta$ -sheet and random coil was transformed to  $\alpha$ -helix and  $\beta$ -turn. Other researchers reported similar results (Tang & Ma, 2009; Wang et al., 2011b; Martínez et al., 2017). After further high HHP treatment (at 500 MPa),  $\alpha$ -helix,  $\beta$ -sheet and random coil contents of SPI were reduced and their  $\beta$ -turn content increased. Tabilo-Munizaga et al. (2014) found that the loss of  $\alpha$ -helix content of protein in bottled white wine under 450 MPa led to the changes in electrostatic interactions and hydrogen bond stability. The result indicated that the unfolded SPI had undergone a rebuilding process of secondary structures, since  $\beta$ -turn content significantly increased after HHP treatment (500 MPa). Generally, the amide I band is due to the C=O stretching vibrations with certain N-H bending and C-H stretching patterns, which reflect intra- or intermolecular effects

and the secondary structures (Militello et al., 2004; Tang & Ma, 2009; Tabilo-Munizaga et al., 2014). The results inferred that SPI unfolded and denatured in the initial stage of HHP treatment, damaged the hydrophobic group or hydrogen bonding mode of protein, undergone a reaggregation of secondary structure during the later stage of HHP treatment. Similar observation was reported for whole wheat flour doughs treated by high pressure (Ahmed et al., 2018).

Most of the  $\beta$ -turn lies on the surface of protein molecule, altering the direction of the peptide chain. The  $\beta$ -turn is fairly abundant in globular proteins, accounting for about a quarter of the total amino acid residues (Whitford, 2005). The HHP treatment made the protein peptide chain expand, the secondary structure change, and the non-covalent interactions (hydrogen bonds, ion and hydrophobic interaction) of protein molecules alter. Then the protein molecules showed the ordered supramolecular structure with the molecular interaction (Balci & Wilbey, 1999; Wang et al., 2011b).

### 3.2 Fluorescence spectra analysis

Fluorescence spectroscopy is a useful technique for researching tertiary structure of protein. Conformational changes in the tertiary structure of SPI caused by the molecular environment changes. Changes in the fluorescence spectra of protein result from the environment of the tryptophan (Trp), phenylalanine and tyrosine groups (Zhu et al., 2018). The fluorescence spectra of untreated and HHP treated SPI samples described in Figure 3 were obviously different. Compared with the control, the maximum

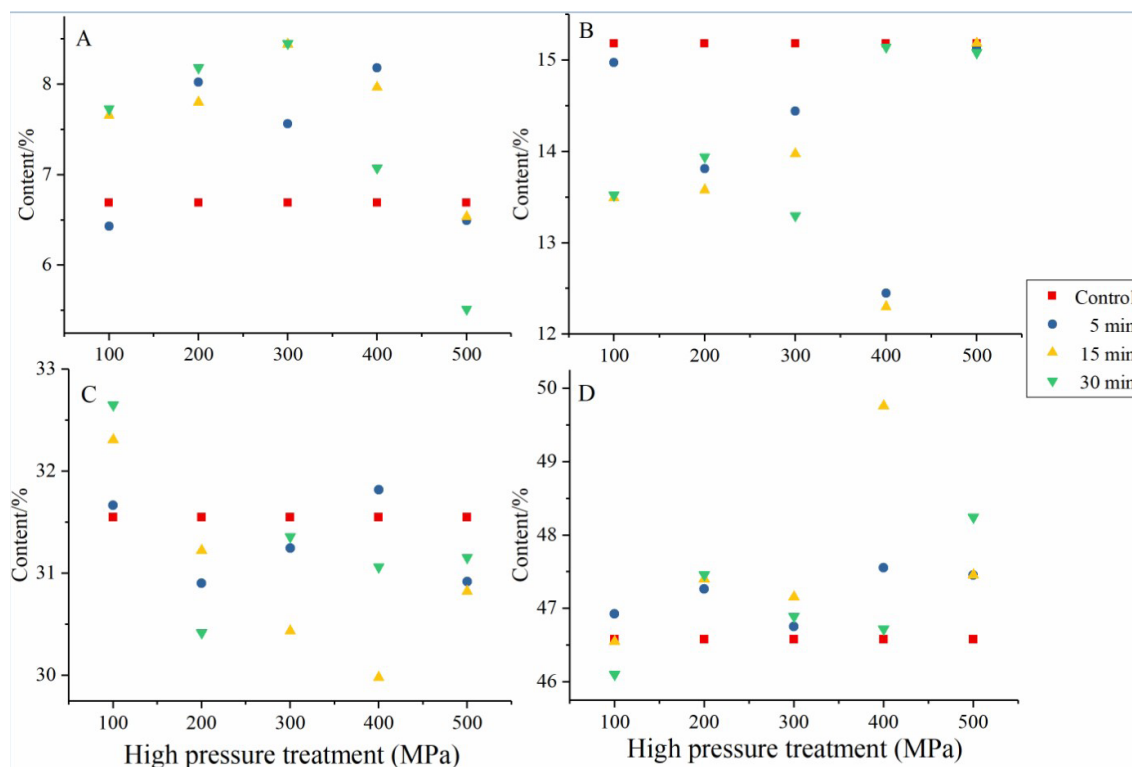


**Figure 2.** Effects of HHP treatment on secondary structure composition of SPI (A:  $\alpha$ -helix, B: random coil, C:  $\beta$ -sheet, D:  $\beta$ -turn).

wave length ( $\lambda_{\max}$ ) and fluorescence intensity of SPI were greatly changed. If the  $\lambda_{\max}$  is greater than 330 nm, then Trp is defined as a “polar” environment, whereas the opposite is a “non-polar” environment (Zhao et al., 2019). Trp of the samples were determined to be in a “polar” environment. The  $\lambda_{\max}$  of HHP-treated samples had hypochromic shift (from 343 nm to 339-342 nm), which indicating that the microenvironment of Trp residues was altered. This might be attributed to the change in the internal hydrophobic interactions of SPI molecules. These results indicated that the tertiary structure of SPI had been destroyed after HHP treatment.

From the Figure 3, the fluorescence intensity decreased markedly after HHP treatment, showing that the fluorophore residue of SPI was buried in the molecules under applied pressure. Wang et al. (2008) reported that the exposed hydrophobic groups may re-associate or aggregate to form a more stable structure. As pressure increased to 300-400 MPa, the fluorescence intensity of SPI treated for 30 min increased significantly, and processed at 500 MPa for 5 min, the fluorescence intensity increased slightly compared with that of the control sample. The hydrophobic groups of protein were exposed on the surface at medium pressure for long-time or high pressure for short time treatment, and the fluorescence quantum yield of Trp residue decreased as their exposure to the solvent increased (Tang & Ma, 2009). Similar observations were reported for SPI and soybean seed ferritin after HHP treatment (Wang et al., 2008; Zhang et al., 2012). The protein primary structure is kept together by covalent bonds, and hydrophobic interactions, hydrogens bonds and

electrostatic interactions dominate the secondary and tertiary structures (Munir et al., 2019). The results showed that HHP treatment affected the tertiary structure of SPI.

### 3.3 Effective diameter analysis

As can be seen in Figure 4, the particle size of the SPI was significantly reduced after HHP treatment. The effective diameter range of the SPI dispersions was from 192.70 nm to 215.30 nm, while that of the untreated protein was 217.20 nm. Ahmed et al. (2018) found that HHP-treatment significantly reduced the particle-size distribution of kidney bean protein isolate. Moreover, with pressure (200-400 MPa) treated prolong time, protein particles were broken up into smaller aggregates (5 min), while the processing time was increased, the small SPI aggregation formed into large polymer (15 min), then SPI was broken into smaller particle size polymers after time-consuming processing treatment (30 min). The reversibility of the increase in effective diameter after time-consuming processing treatment may be the result of reformation of a large number of protein micellar particles with a size smaller than these aggregates (Huppertz et al., 2006). HHP treatment caused different degrees of changes in the secondary and tertiary structures of proteins, resulting in loose structure and changes in intermolecular hydrogen bonds and hydrophobicity, thus denaturing proteins and changing their functional characteristics (Whitford, 2005).

### 3.4 Effects of HHP treatment on $\zeta$ -potential of SPI

The surface charge characteristics of protein particle in solution were analyzed by  $\zeta$ -potential. Generally, the negative net charge is due to aspartic and glutamic acid and the positive net electronic charge attributes to lysine and histidine acid (Liu et al., 2015). If more positively charged amino acids are present than negatively charged amino acids, the  $\zeta$ -potential of a protein solution is positive (Bouzid et al., 2008).

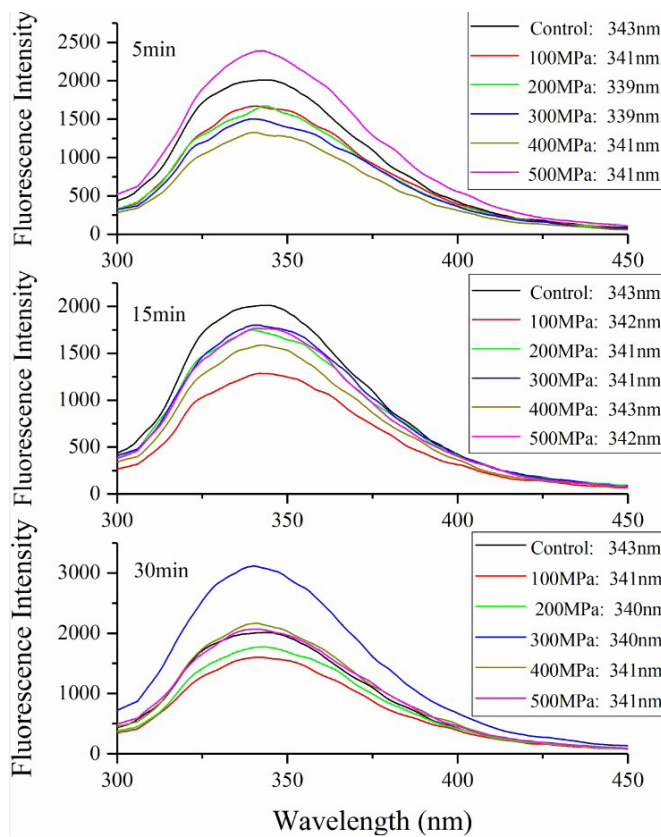


Figure 3. Fluorescence spectra of SPI after HHP treatment.

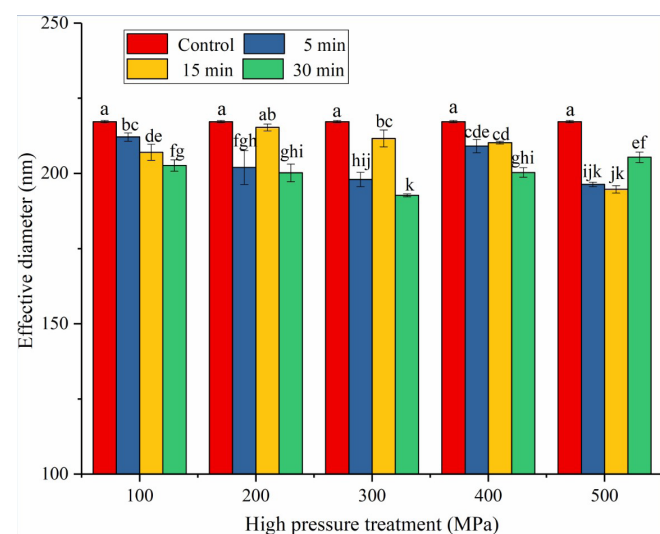
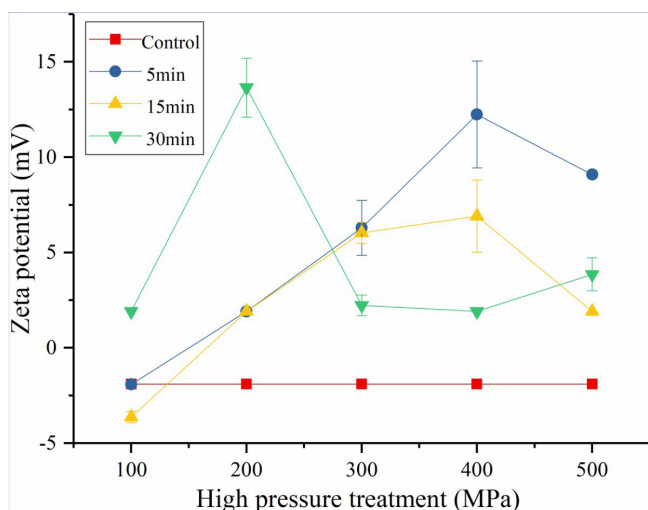


Figure 4. Effective diameter for SPI samples. Data were the averages of three replications  $\pm$  standard deviation. Data with the letter were not significantly different within the same concentration at  $P < 0.05$ .

SPI is a representative ampholyte with a bunch of non-polar and polar (Amino, carboxyl, hydroxyl) groups on the side chain (Wang et al., 2022). As shown in Figure 5, the highest  $\zeta$ -potential (13.65 mV) was got at 200 MPa (30 min), due to the exposure of the positively charged groups containing lysine and histidine on the SPI surface. The  $\zeta$ -potentials of the samples treated at 100 MPa for 5 and 15 min were negative, indicating that more negatively charged amino acids were exposed on the protein surface. Meanwhile the  $\zeta$ -potentials of the other samples were positive. The surface charge of the protein particles increased, suggesting that the original dense spherical structure of the protein was destroyed, and the protein molecules dispersed into aggregations of different sizes after HHP treatment. The high pressure transferred to the protein evenly and quickly by water used as transferring agent during HHP treatment. The secondary bonds (ionic bond, hydrogen bond and hydrophobic bond and so on) of the protein molecules were damaged, exposing the hydrophobic groups and polar groups, then the protein had electric charges on the surface. The Zeta potential value of SPI firstly increased and then decreased with the increasing of processing pressure and time in Figure 5. This suggested that the intermolecular hydrophobic interaction improved after HHP treatment for higher pressure and long time, and protein molecular rearranged to form large aggregations, burying charged groups in the molecule (Wang et al., 2008). After the pressure disappeared, the molecular structure of denatured protein changed, then the functional properties of proteins were improved. The effect of HHP treatment was related to the pressure, processing time, protein type, structure and solvent properties and so on (Murchie et al., 2005). Generally, the potential value is greater than 25 mV or less than -25 mV, the solution is relatively stable (Ortiz & Wagner, 2002). The highest  $\zeta$ -potential of sample was 13.65 mV, indicating the SPI molecules after HHP treatment in solution were still in an unstable state. The changes of protein caused by 100-250 MPa pressure was temporary and reversible, while the protein treated with higher pressure ( $> 300$  MPa) caused irreversible change of molecular conformation (Neetoo & Chen, 2012).



**Figure 5.** Zeta-potential value of HHP-treated SPI. Data were the averages of three replications  $\pm$  standard deviation.

### 3.5 Scanning electron microscopy

The effect of HHP treatment on the microstructure of protein was investigated by SEM. Figure 6 showed the SEM images of samples with 200-fold and 2000-fold magnification. Indeed, the untreated SPI particles were compact with smooth surfaces, spherical and nonporous (Figure 6A). After HHP treatment with different pressure and time, samples were large irregular in shape, agglomerated tightly lamellar structure, and some pores were developed on the surfaces (Figure 6B-6D). This indicated that SPI was impacted into countless irregular small spheroidicity and crosslinked together under HHP treatment, and the spherical particles of protein almost disappeared. This was similar to the morphological changes of kidney bean isolate treated with HHP treatment (Ahmed et al., 2018). As can be seen from the SEM images (E-H) with 2000-fold magnification in Figure 6, the structure of SPI became loose after HHP treatment, and formed molecule aggregation. When the pressure was increased, the molecular particles size became smaller, which was consistent with the change of particle size of SPI (Section 3.4). The surface was uneven after pressure treatment and became smoother at higher pressure (500 MPa). The results showed that globular protein changed into non-spherical particles after HHP treatment, the specific surface area of SPI increased, and the intermolecular electrostatic attraction played a major role in forming large size protein particles.

### 3.6 Light scattering analysis

Light scattering technique is an useful method for characterization of physical properties of macromolecules, including static and dynamic light scattering. The combination of SLS and DLS can apply to characterize the SPI solution conformation. SPI samples after HHP treatment were dissolved in water, protein aggregates were showed for the strong intermolecular forces (Li et al., 2006). The angular dependence of hydrodynamic radius ( $R_h$ ) got from DLS, and Weight-average molecular weight ( $M_w$ ), the z-average mean radius of gyration ( $R_g$ ), and the second virial coefficient ( $A_2$ ) of molecular parameters were obtained from SLS. Light scattering is an efficient and rapid method for determination of protein aggregation behavior. The light scattering data of SPI samples after HHP treatment were shown in Table 1.

SLS measurements were measured for the determination of the size and the molecular weight of SPI. The Berry plot of SPI samples in dilute solution (concentrations ranging from 0.03 to 0.20 mg/mL) at angles from 30 to 120 was shown in Table 1. The  $M_w$  of samples significantly increased after HHP treatment. The  $M_w$  of untreated SPI was  $2.89 \times 10^6$  g/mol, while that of SPI treated at 100 MPa for 30 min increased to  $3.11 \times 10^8$  g/mol due to protein aggregates. The  $M_w$  decreased with the pressure increasing, and the  $M_w$  value after 300 MPa (15 min) treatment became  $2.9 \times 10^6$  g/mol. When the pressure continued to increase, the  $M_w$  increased, and the  $M_w$  of SPI treated at 500 MPa (5 min) became  $1.3 \times 10^8$  g/mol. The  $M_w$  of SPI was  $2.57 \times 10^8$  g/mol after 100 MPa HHP treatment for 5 min, decreased to  $8.2 \times 10^7$  g/mol after HHP treatment for 15 min, while increased to  $3.11 \times 10^8$  g/mol after 30 min. The  $M_w$  of SPI (100 MPa) decreased first and then increased with the extension of processing time. The results indicated that the structure of SPI was destroyed and

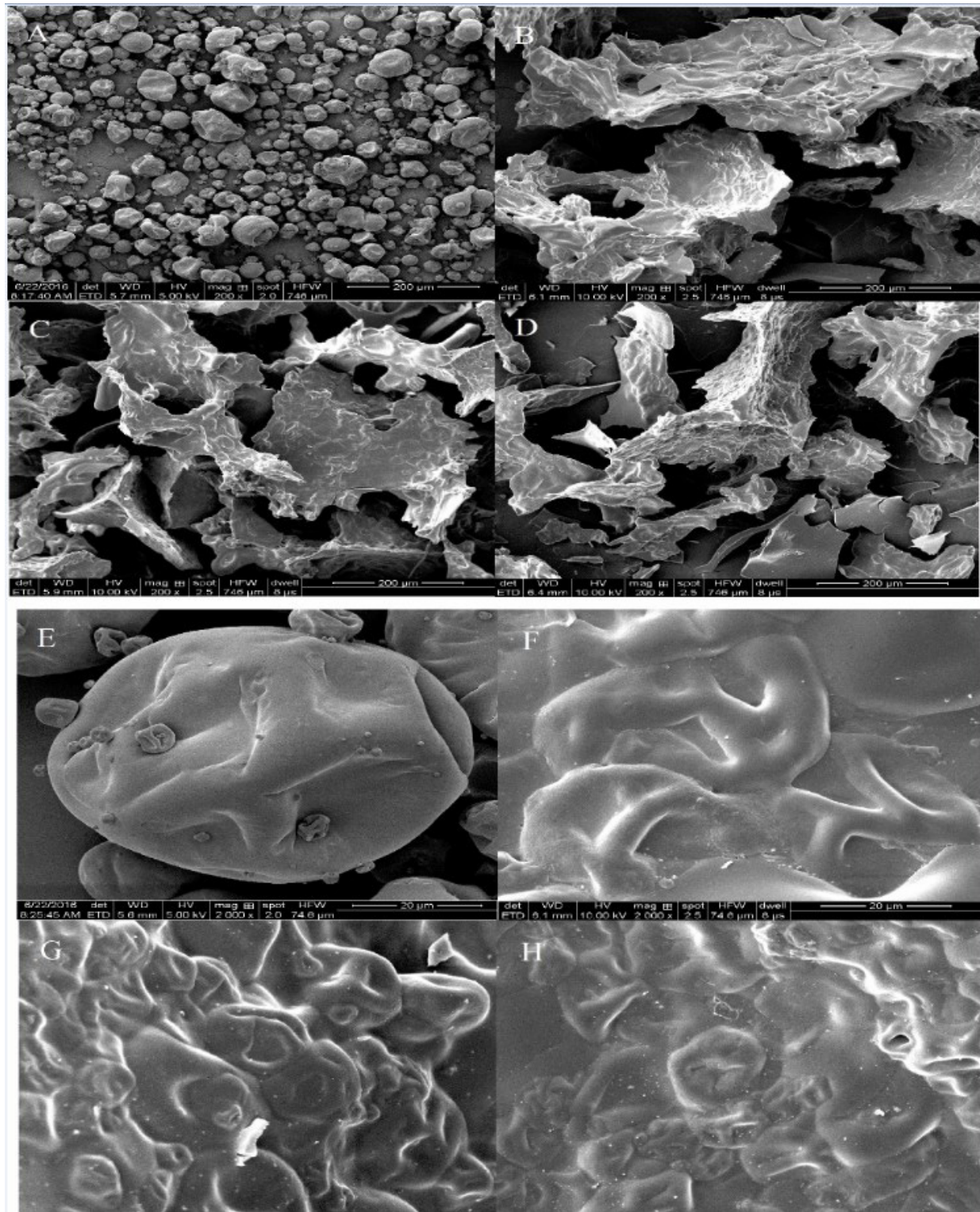


**Figure 6.** Scanning electron micrographs of SPI formed from non-HHP treated SPI (A,E), HPH-100MPa-10min SPI (B,F), HHP-300MPa-5min SPI (C,G) and HHP- 500MPa-30min SPI (D,H) (A-D, 200 fold magnification; E-H, 2000 fold magnification).

assembled into macromolecules. Lower pressure (100 MPa) and higher pressure (500 MPa) treated SPI formed large molecular weight aggregates, and the smaller molecular weight polymer was generated at medium pressure (300 MPa), suggesting that

the intermolecular hydrogen bond, electrostatic interaction, disulfide bond, hydrophobic interaction, and the thermal effect of water of SPI after HHP treatment jointly formed different molecular weight of aggregations.

**Table 1.** Summaries of dynamic and static light scattering data on the soluble aggregates in the SPI aqueous solutions after HHP treatment.

Entry	$M_w$ (g/mol)	$R_g$ (nm)	$R_h$ (nm)	$A_2$	$p (R_g/R_h)$	Structure
Control	$2.89 \pm 0.17 \times 10^6$	$96 \pm 5.4$	122.97	$-3.28 \pm 0.65 \times 10^{-4}$	0.78	Hard sphere
100 MPa-5 min	$2.57 \pm 0.39 \times 10^8$	$100 \pm 18$	95.99	$8 \pm 3.8 \times 10^{-7}$	1.04	Hollow sphere
100 MPa-15 min	$8.2 \pm 0.33 \times 10^7$	$93 \pm 4.8$	89.86	$4.31 \pm 0.8 \times 10^{-6}$	1.03	Hollow sphere
100 MPa-30 min	$3.11 \pm 0.2 \times 10^8$	$96.1 \pm 7.4$	90.63	$4.23 \pm 0.38 \times 10^{-6}$	1.06	Hollow sphere
200 MPa-5 min	$5.3 \pm 1.3 \times 10^6$	$148 \pm 20$	188.69	$-3.52 \pm 0.83 \times 10^{-4}$	0.78	Hard sphere
200 MPa-15 min	$9.3 \pm 4.2 \times 10^6$	$152 \pm 37$	173.34	$-1.8 \pm 0.38 \times 10^{-4}$	0.93	Hollow sphere
200 MPa-30 min	$6.8 \pm 5.9 \times 10^7$	$351 \pm 93$	158.39	$4 \pm 11 \times 10^{-6}$	2.22	GCP
300 MPa-5 min	$7.7 \pm 5.2 \times 10^7$	$260 \pm 60$	176.29	$6.7 \pm 6.6 \times 10^{-6}$	1.47	GCM
300 MPa-15 min	$2.9 \pm 1.9 \times 10^6$	$169 \pm 52$	175.87	$-1.13 \pm 0.53 \times 10^{-6}$	0.96	Hollow sphere
300 MPa-30 min	$9.5 \pm 5.3 \times 10^6$	$161 \pm 52$	192.58	$-4.5 \pm 2.2 \times 10^{-4}$	0.84	Hard sphere
400 MPa-5 min	$2.53 \pm 0.9 \times 10^7$	$199 \pm 29$	201.73	$-5 \pm 4.2 \times 10^{-6}$	0.99	Hollow sphere
400 MPa-15 min	$5.1 \pm 2.8 \times 10^7$	$214 \pm 46$	210.93	$-5 \pm 17 \times 10^{-5}$	1.01	Hollow sphere
400 MPa-30 min	$9.1 \pm 7.1 \times 10^7$	$195 \pm 64$	138.21	$-8 \pm 570 \times 10^{-7}$	0.8	Hard sphere
500 MPa-5 min	$1.3 \pm 1.4 \times 10^8$	$259 \pm 98$	216.19	$4.0 \pm 4.6 \times 10^{-5}$	1.2	GCM
500 MPa-15 min	$4.1 \pm 2.8 \times 10^7$	$201 \pm 57$	190.8	$-1.5 \pm 1.8 \times 10^{-4}$	1.05	Hollow sphere
500 MPa-30 min	$8.8 \pm 6.7 \times 10^7$	$203 \pm 64$	197.59	$2 \pm 20 \times 10^{-5}$	1.03	Hollow sphere

Weight-average molecular weight ( $M_w$ ); z-average mean radius of gyration ( $R_g$ ); hydrodynamic radius ( $R_h$ ); the second virial coefficient ( $A_2$ ); Gaussian coil, monodisperse (GCM); Gaussian coil, polydisperse (GCP).

$A_2$  is a measure of the interaction between the solvent and the polymer (Li et al., 2006). The small and positive  $A_2$  value further confirmed that the solubility of protein was obviously improved after 100 MPa HHP treatment. Protein molecules depolymerize into subunits after HHP treatment with the internal hydrophilic groups exposed, increasing the ability to bind with water, thus improving the solubility of proteins. As the pressure increased, the  $A_2$  value of SPI were negative, indicating the solubility of protein decreased. Wang et al. (2008) showed that HHP treatment at 200-600 MPa resulted in a slight but gradual decline in solubility of SPI. Chapleau & Lamballerie-Anton (2003) found that a decrease of protein solubility of lupin proteins revealed a partial dissociation of monomers. The results suggested that the negatively charged amino acids were exposed on the protein surface at low pressure, and electrostatic repulsion was the main force between protein molecules.

Compared to untreated protein, the  $R_g$  of protein treated at 100 MPa showed little change. The  $R_g$  of SPI increased with the increasing pressure. The  $R_g$  of samples treated at 200 MPa for 30 min was higher than other samples. The results might due to noncovalent interactions, such as hydrophobic interactions and electrostatic forces, might contribute to aggregation of SPI. This showed that the secondary structure of protein was destroyed after HHP treatment, the partial polar and hydrophobic groups was exposed.

The  $R_h$  distribution were detected in SPI water solution after HHP treatment. In the present study, the  $R_h$  value of untreated SPI was calculated to be 122.97 nm, while the  $R_h$  value of samples treated at 100 MPa (15 min) reduced obviously to 89.86 nm. As the pressure continued to increase, the  $R_h$  value of protein

increased, and the largest  $R_h$  value was obtained in HHP-treated SPI at 500 MPa for 5 min. The  $R_h$  of protein decreased with the treatment time prolonging. The results indicated that the protein peptide chain dissociated and unfolded, then intermolecular interactions led to the formation of polymers with different molecular weights and morphologies.

The parameter  $p$  was used to characterize the morphological changes of SPI in solution, which is the ratio of  $R_g$  to  $R_h$ . Generally, the  $p$  value decreased in polydispersity counteracts the effect of branching, and an increase with decreasing branching density (Zhao et al., 2018). The  $p$  values of the control was 0.78, which is predicted for a hard sphere. The  $p$  values of HHP-treated SPI were 0.98-1.06, which is predicted for hollow sphere. But the higher  $p$  values (2.22 and 1.47) were obtained for samples which were treated 200 MPa (30 min) and 300 MPa (5 min), which are predicted polydisperse and monodisperse gaussian coils; the structure of samples treated at 200 MPa (5 min), 300 MPa (5 min) and 400 MPa (30 min) were the same as the control. The results indicated that most of the structures of SPI treated HHP treatment were hollow spheres. The globular structure was unfolded, compressed, and then became a flat ball; the hydrophobic region inside the molecule exposed, SPI molecules contacted with each other and interacted with water, thus formed large hollow spherical aggregates.

This suggested that the SPI structure changed from hard sphere to hollow spheres after HHP treatment. The globular structure of SPI was unfolded, and the polypeptide chain depolymerized, then proteins was compressed at high pressure, then became a flat ball; thus formed large hollow spherical aggregates via hydrogen bonding, electrostatic and hydrophobic interaction.

Therefore, the hydration patterns of the protein would bring remarkable effect on the structural dynamic properties with different pressure treatments.

### 3.7 Foaming properties

The foaming ability (FA) and foaming stability (FS) of SPI at the same concentration of 4% (w/v) were described in Figure 7. The FA of HHP treated SPI (200 MPa, 5 min) was 0.68-fold higher than that of untreated SPI (Figure 7A). With the extension of time, the FA of HHP-treated samples increased. This suggested that HHP treatment could improve the FA of SPI (more foam volume and smaller bubble sizes) than the untreated samples, as HHP treatment induced partial unfolding of the protein polar groups and hydrophobic groups, forming viscoelastic films at air-water interface, surrounding the gas to form foam. Krešić et al. (2006) found that high-pressure treatments could improve the foaming behavior of WPI due to the increase in the lots of available surface-active residues. With the pressure increasing, the FA of the protein decreased attribute to insoluble aggregates. The results suggested that the decrease in soluble protein weaken the interaction between protein molecules, and reduced the number of protein useful for film formation. It was found that high-pressure treatments could improve the foaming behavior of whey protein isolate and kidney bean protein isolate due to the increase in the lots of available surface-active residues (Krešić et al., 2006; Ahmed et al., 2018). High pressure gave rise

to a partial degeneration by expanding molecular structure of the protein, affecting its functional characteristics (Qiu et al., 2014). Compared with the untreated protein solution, the foam of SPI solution treated HHP treatment was more delicate, less fragile, smaller in size and less likely to coalesced and aggregate. Generally speaking, the foamability of protein is closely related to the surface hydrophobicity of protein. On the basis of the SPI fluorescence spectra, hydrophobic groups hidden inside proteins were exposed after HHP treatment, leading to a fast extension and adsorption at gas-liquid interface, then forming a cohesive viscoelastic films. The pressurized protein became more flexible, and provided enough energy to bubble, then the foamability of protein was improved.

### 3.8 Degree of hydrolysis of SPI hydrolysates

As shown in Figure 8A, the DH of SPI hydrolysates was significantly changed after HHP treatment compared to that of untreated SPI hydrolysates. The DH of the control was 9.53%, and the lowest DH of SPI treated at 200 MPa for 30 min was 21.26%. The DH of samples decreased with the pressure up to 300 MPa, and increased with the pressure up to 500 MPa, the DH reached 24.93% after HHP treatment at 500 MPa for 15 or 30 min. Zhang & Mu (2017) found that the DH of sweet potato protein hydrolysates increased significantly, with the highest value of 31.68% treated at 300 MPa for 60 min. The DH of chickpea protein isolates hydrolyzed at high pressure (100-300 MPa) was significantly improved (Zhang et al.,

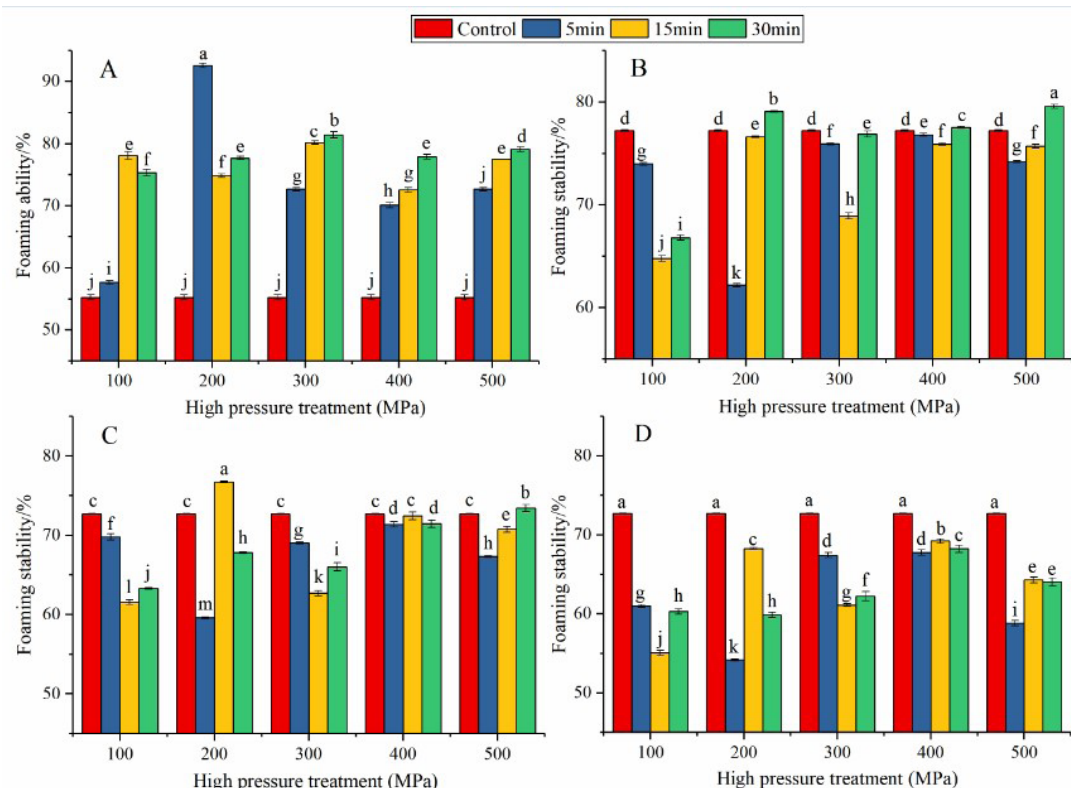


**Figure 7.** Effect of HHP treatment on foam ability (A) and foam stability of SPI (B: Standing-10min, C: Standing-20min, D: Standing-30min). Data were the averages of three replications  $\pm$  standard deviation. Data with the letter were not significantly different within the same concentration at  $P < 0.05$ .

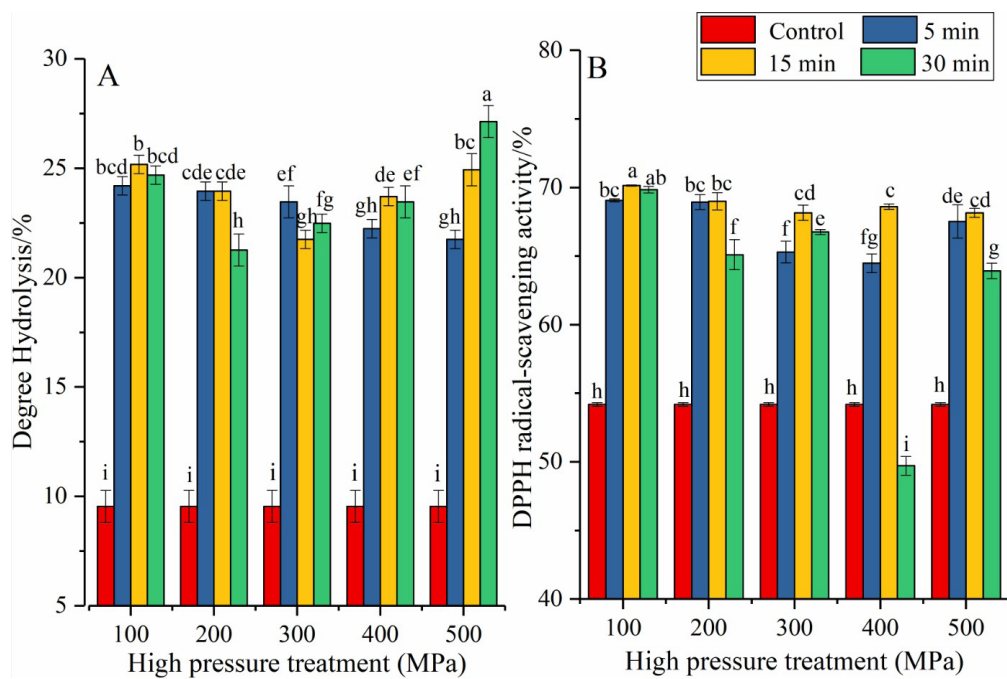


**Figure 8.** Effect of pretreatment on enzymatic hydrolysis and DPPH radical-scavenging activity of the SPI hydrolysates. Data were the averages of three replications  $\pm$  standard deviation. Data with the letter were not significantly different within the same concentration at  $P < 0.05$ .

2012). Ambrosi et al. (2016) reported that the maximum DH of the samples treated at 400 MPa for 30 min were about 17%. The results showed that high-pressure destroyed the secondary and tertiary structure of protein, then more enzymes' sensitive sites were exposed, which improved the enzymatic hydrolysis (Belloque et al., 2007). From the results, we concluded that high pressure treatment enhanced the enzymatic hydrolysis of SPI, and some key parameters such as pressure and treated time must be measured and controlled for appropriate hydrolysis. Moreover, the duration of hydrolysis is vital since it is directly related to the degree of hydrolysis, which influences amino acid composition and the bioactivities of the SPI hydrolysates.

### 3.9 Antioxidant activity of SPI hydrolysates

Figure 8B illustrated the DPPH radical-scavenging activity of various SPI samples, which were prepared by HHP treatment at different pressures. Compared with untreated SPI hydrolysates, high pressure significantly increased the DPPH radical-scavenging activity of SPI hydrolysates. The maximum antioxidant activity of sample hydrolysates was obtained by HHP-treated SPI at 100 MPa for 15 min (70.15%). The antioxidant activity of proteins decreased with the increasing pressure, due to non-reversible SPI aggregation at higher pressure. Zhang & Mu (2017) previously reported that high-pressure treatment at 200 MPa for 20 min resulted in chickpea protein isolates products with high antioxidant activity. Guan et al. (2018) noted that the HHP treatment of SPI at 200 MPa led to a fairly greater accumulation of peptides with high antioxidant activities. The results showed that proper HHP pressure pretreatment of protein and protease hydrolysis was beneficial to obtain SPI antioxidant peptide, and the electron donor ability of the peptide was improved.

## 4 Conclusion

HHP-treatment of SPI had an important impact on the protein denaturation resulting changes in functional and antioxidant properties. Changes in the protein secondary and tertiary structures were evidenced by shifts in the main bands of SPI. A reduction of particle sizes in SPI was observed, which was pressure dependent. HHP also caused significant changes in the surface morphology and zeta potential of SPI with pressure level. Dynamic and static light scattering demonstrated that HHP-treated protein samples formed large hollow spherical aggregates, which might be attribute to fragmentation, denaturation, and aggregation of SPI. Under these conditions, HHP treatment could influence the protein foaming and antioxidant properties, which depends mostly on the changes of their primary structure. HHP treatment improved the values of the DH in SPI during pressure processes, which were increased the protein maximum exposure to the attack of protease. The functional and antioxidant properties of SPI were improved due to the protein structural changes, which induced further peptide bonds cleavage as the combination of HHP treatment and enzymatic hydrolysis were applied. The results of this paper supply the theory basis and direction for the SPI development and will be beneficial to promote comprehensive utilization of SPI. Nevertheless, it also needs to continue to study the completely denatured SPI and understand the related change in structural and functional properties.

## Acknowledgements

The authors would like to thank Weifang University of Science and Technology and Natural Science Foundation of Shandong Province (ZR2020QC222) for financial support.

## References

- Ahmed, J., Al-Ruwaih, N., Mulla, M., & Rahman, M. H. (2018). Effect of high pressure treatment on functional, rheological and structural properties of kidney bean protein isolate. *Lebensmittel-Wissenschaft + Technologie*, 91, 191-197. <http://dx.doi.org/10.1016/j.lwt.2018.01.054>.
- Ahmed, J., Ramaswamy, H. S., Ayad, A., & Alli, I. (2008). Thermal and dynamic rheology of insoluble starch from Basmati rice. *Food Hydrocolloids*, 22(2), 278-287. <http://dx.doi.org/10.1016/j.foodhyd.2006.11.014>.
- Ambrosi, V., Polenta, G., Gonzalez, C. B., Ferrari, G., & Maresca, P. (2016). High hydrostatic pressure assisted enzymatic hydrolysis of whey proteins. *Innovative Food Science & Emerging Technologies*, 38, 294-301. <http://dx.doi.org/10.1016/j.ifset.2016.05.009>.
- Balci, A. T., & Wilbey, A. (1999). High pressure processing of milk - the first 100 years in the development of a new technology. *International Journal of Dairy Technology*, 52(4), 149-155. <http://dx.doi.org/10.1111/j.1471-0307.1999.tb02858.x>.
- Belloque, J., Chicón, R., & López-Fandiño, R. (2007). Unfolding and refolding of  $\beta$ -lactoglobulin subjected to high hydrostatic pressure at different pH values and temperatures and its influence on proteolysis. *Journal of Agricultural and Food Chemistry*, 55(13), 5282-5288. <http://dx.doi.org/10.1021/jf070170w>. PMid:17542606.
- Bogahawaththa, D., Buckow, R., Chandrapala, J., & Vasiljevic, T. (2018). Comparison between thermal pasteurization and high pressure processing of bovine skim milk in relation to denaturation and immunogenicity of native milk proteins. *Innovative Food Science & Emerging Technologies*, 47, 301-308. <http://dx.doi.org/10.1016/j.ifset.2018.03.016>.
- Bouzid, H., Rabiller-Baudry, M., Paugam, L., Rousseau, F., Derriche, Z., & Bettahar, N. E. (2008). Impact of zeta potential and size of caseins as precursors of fouling deposit on limiting and critical fluxes in spiral ultrafiltration of modified skim milks. *Journal of Membrane Science*, 314(1-2), 67-75. <http://dx.doi.org/10.1016/j.memsci.2008.01.028>.
- Chapleau, N., & Lamballerie-Anton, M. (2003). Improvement of emulsifying properties of lupin proteins by high-pressure induced aggregation. *Food Hydrocolloids*, 17(3), 273-280. [http://dx.doi.org/10.1016/S0268-005X\(02\)00077-2](http://dx.doi.org/10.1016/S0268-005X(02)00077-2).
- Cheftel, J. C. (1992). Effects of high hydrostatic pressure on food constituents: an overview. In C. Balny, R. Hayashi, K. Heremans & P. Masson (Eds.), *High pressure and biotechnology* (pp. 195-209). Montrouge: John Libbey Eurotext.
- Furtado, G. F., Mantovani, R. A., Consoli, L., Hubinger, M. D., & Cunha, R. L. (2017). Structural and emulsifying properties of sodium caseinate and lactoferrin influenced by ultrasound process. *Food Hydrocolloids*, 63, 178-188. <http://dx.doi.org/10.1016/j.foodhyd.2016.08.038>.
- Guan, H., Diao, X., Jiang, F., Han, J., & Kong, B. (2018). The enzymatic hydrolysis of soy protein isolate by Corolase PP under high hydrostatic pressure and its effect on bioactivity and characteristics of hydrolysates. *Food Chemistry*, 245, 89-96. <http://dx.doi.org/10.1016/j.foodchem.2017.08.081>. PMid:29287456.
- Huppertz, T., Fox, P. F., & Kelly, A. L. (2004). High pressure treatment of bovine milk: effects on casein micelles and whey proteins. *The Journal of Dairy Research*, 71(1), 97-106. <http://dx.doi.org/10.1017/S002202990300640X>. PMid:15068072.
- Huppertz, T., Fox, P. F., Kruif, K. G., & Kelly, A. L. (2006). High pressure-induced changes in bovine milk proteins: a review. *Biochimica et Biophysica Acta (BBA)-Proteins and Proteomics*, 1764(3), 593-598. <http://dx.doi.org/10.1016/j.bbapap.2005.11.010>. PMid:16410058.
- Indyk, H. E., Williams, J. W., & Patel, H. A. (2008). Analysis of denaturation of bovine IgG by heat and high pressure using an optical biosensor. *International Dairy Journal*, 18(4), 359-366. <http://dx.doi.org/10.1016/j.idairyj.2007.10.004>.
- Jia, J., Ma, H., Zhao, W., Wang, Z., Tian, W., Luo, L., & He, R. (2010). The use of ultrasound for enzymatic preparation of ACE-inhibitory peptides from wheat germ protein. *Food Chemistry*, 119(1), 336-342. <http://dx.doi.org/10.1016/j.foodchem.2009.06.036>.
- Krešić, G., Lelas, V., Herceg, Z., & Režek, A. (2006). Effects of high pressure on functionality of whey protein concentrate and whey protein isolate. *Dairy Science & Technology*, 86(4), 303-315. <http://dx.doi.org/10.1051/lait:2006012>.
- Li, W., Wang, Q., Cui, S. W., Huang, X., & Kakuda, Y. (2006). Elimination of aggregates of (1 $\rightarrow$ 3) (1 $\rightarrow$ 4)-beta-D-glucan in dilute solutions for light scattering and size exclusion chromatography study. *Food Hydrocolloids*, 20(2-3), 361-368. <http://dx.doi.org/10.1016/j.foodhyd.2005.03.018>.
- Liu, Q., Lu, Y., Han, J., Chen, Q., & Kong, B. (2015). Structure-modification by moderate oxidation in hydroxyl radical-generating systems promote the emulsifying properties of soy protein isolate. *Food Structure*, 6, 21-28. <http://dx.doi.org/10.1016/j.foostr.2015.10.001>.
- López-Fandiño, R. (2006). High pressure-induced changes in milk proteins and possible applications in dairy technology. *International Dairy Journal*, 16(10), 1119-1131. <http://dx.doi.org/10.1016/j.idairyj.2005.11.007>.
- Martínez, M. A., Velazquez, G., Cando, D., Núñez-Flores, R., Borderías, A. J., & Moreno, H. M. (2017). Effects of high pressure processing on protein fractions of blue crab (*Callinectes sapidus*) meat. *Innovative Food Science & Emerging Technologies*, 41, 323-329. <http://dx.doi.org/10.1016/j.ifset.2017.04.010>.
- Militello, V., Casarino, C., Emanuele, A., Giostra, A., Pullara, F., & Leone, M. (2004). Aggregation kinetics of bovine serum albumin studied by FTIR spectroscopy and light scattering. *Biophysical Chemistry*, 107(2), 175-187. <http://dx.doi.org/10.1016/j.bpc.2003.09.004>. PMid:14962598.
- Munir, M., Nadeem, M., Qureshi, T. M., Leong, T. S. H., Gamlath, C. J., Martin, G. J. O., & Ashokkumar, M. (2019). Effects of high pressure, microwave and ultrasound processing on proteins and enzyme activity in dairy systems-a review. *Innovative Food Science & Emerging Technologies*, 57, 102192. <http://dx.doi.org/10.1016/j.ifset.2019.102192>.
- Murchie, L., Cruz-Romero, M., Kerry, J. P., Linton, M., Patterson, M. F., & Smiddy, M. (2005). High pressure processing of shellfish: a review of microbiological and other quality aspects. *Innovative Food Science & Emerging Technologies*, 6(3), 257-270. <http://dx.doi.org/10.1016/j.ifset.2005.04.001>.
- Neetoo, H., & Chen, H. (2012). Progress in food preservation. In R. Bhat, A. K. Alias & G. Paliyath (Eds.), *Application of high hydrostatic pressure technology for processing and preservation of foods* (pp. 247-276). New York: John Wiley & Sons, Ltd.
- Nogueira, A. C., Aquino, R. K. N., & Steel, C. J. (2022). Empirical rheology of wheat flour doughs with pea, soybean and whey protein isolates. *Food Science and Technology*, 42, e23921. <http://dx.doi.org/10.1590/fst.23921>.
- Ortiz, S. E. M., & Wagner, J. R. (2002). Hydrolysates of native and modified soy protein isolates: structural characteristics, solubility and foaming properties. *Food Research International*, 35(6), 511-518. [http://dx.doi.org/10.1016/S0963-9969\(01\)00149-1](http://dx.doi.org/10.1016/S0963-9969(01)00149-1).
- Peñas, E., Préstamo, G., Baeza, M. L., Martínez-Molero, M. I., & Gomez, R. (2006). Effects of combined high pressure and enzymatic treatments on the hydrolysis and immunoreactivity of dairy whey

- proteins. *International Dairy Journal*, 16(8), 831-839. <http://dx.doi.org/10.1016/j.idairyj.2005.08.009>.
- Puteri, N. E., Astawan, M., Palupi, N. S., Wresdiyati, T., & Takagi, Y. (2018). Characterization of biochemical and functional properties of water-soluble tempe flour. *Food Science and Technology*, 38(Suppl. 1), 147-153. <http://dx.doi.org/10.1590/fst.13017>.
- Qiu, S., Li, Y., Chen, H., Liu, Y., & Yin, L. (2014). Effects of high-pressure homogenization on thermal and electrical properties of wheat starch. *Journal of Food Engineering*, 128, 53-59. <http://dx.doi.org/10.1016/j.jfoodeng.2013.12.011>.
- Shao, Y., Xiong, G., Ling, J., Hu, Y., Shi, L., Qiao, Y., Yu, J., Cui, Y., Liao, L., Wu, W., Li, X., Ding, A., & Wang, L. (2018). Effect of ultra-high pressure treatment on shucking and meat properties of red swamp crayfish (*Procambarus clarkia*). *Lebensmittel-Wissenschaft + Technologie*, 87, 234-240. <http://dx.doi.org/10.1016/j.lwt.2017.07.062>.
- Tabilo-Munizaga, G., Gordon, T. A., Villalobos-Carvajal, R., Moreno-Osorio, L., Salazar, F. N., Pérez-Won, M., & Acuña, S. (2014). Effect of high hydrostatic pressure (HHP) on the protein structure and thermal stability of Sauvignon blanc wine. *Food Chemistry*, 155, 214-220. <http://dx.doi.org/10.1016/j.foodchem.2014.01.051>. PMid:24594177.
- Tang, C., & Ma, C. (2009). Effect of high pressure treatment on aggregation and structural properties of soy protein isolate. *Lebensmittel-Wissenschaft + Technologie*, 42(2), 606-611. <http://dx.doi.org/10.1016/j.lwt.2008.07.012>.
- Torrezan, R., Tham, W. P., Bell, A. E., Frazier, R. A., & Cristianini, M. (2007). Effects of high pressure on functional properties of soy protein. *Food Chemistry*, 104(1), 140-147. <http://dx.doi.org/10.1016/j.foodchem.2006.11.013>.
- Wang, B., Meng, T., Ma, H., Zhang, Y., Li, Y., Jin, J., & Ye, X. (2016). Mechanism study of dual-frequency ultrasound assisted enzymolysis on rapeseed protein by immobilized Alcalase. *Ultrasonics Sonochemistry*, 32, 307-313. <http://dx.doi.org/10.1016/j.ultsonch.2016.03.023>. PMid:27150775.
- Wang, C., Jiang, L., Wei, D., Li, Y., Sui, X., Wang, Z., & Li, D. (2011a). Effect of secondary structure determined by FTIR spectra on surface hydrophobicity of soybean protein isolate. *Procedia Engineering*, 15, 4819-4827. <http://dx.doi.org/10.1016/j.proeng.2011.08.900>.
- Wang, J.-M., Yang, X.-Q., Yin, S.-W., Zhang, Y., Tang, C.-H., Li, B.-S., Yuan, D.-B., & Guo, J. (2011b). Structural rearrangement of ethanol-denatured soy proteins by high hydrostatic pressure treatment. *Journal of Agricultural and Food Chemistry*, 59(13), 7324-7332. <http://dx.doi.org/10.1021/jf201957r>. PMid:21609024.
- Wang, X., Tang, C., Li, B., Yang, X., Li, L., & Ma, C. (2008). Effects of high-pressure treatment on some physicochemical and functional properties of soy protein isolates. *Food Hydrocolloids*, 22(4), 560-567. <http://dx.doi.org/10.1016/j.foodhyd.2007.01.027>.
- Wang, Z. J., Li, B. L., Wang, Z. B., Li, J., Xing, L., Zhou, L. Y., Zou, X. H., & Yin, H. (2022). Analysis of structural changes and anti-inflammatory capacity in soybean protein isolates conjugated with anthocyanins. *Food Science and Technology*, 42, e07922. <http://dx.doi.org/10.1590/fst.07922>.
- Whitford, D. (2005). *Proteins: structure and function*. London: John Wiley & Sons Ltd. Amino acid: the building blocks of proteins, pp. 19-21.
- Xiong, T., Xiong, W., Ge, M., Xia, J., Li, B., & Chen, Y. (2018). Effect of high intensity ultrasound on structure and foaming properties of pea protein isolate. *Food Research International*, 109, 260-267. <http://dx.doi.org/10.1016/j.foodres.2018.04.044>. PMid:29803449.
- Yuan, B., Ren, J., Zhao, M., Luo, D., & Gu, L. (2012). Effects of limited enzymatic hydrolysis with pepsin and on the functional properties of soybean protein isolate. *Lebensmittel-Wissenschaft + Technologie*, 46(2), 453-459. <http://dx.doi.org/10.1016/j.lwt.2011.12.001>.
- Zhang, M., & Mu, T. (2017). Identification and characterization of antioxidant peptides from sweet potato protein hydrolysates by Alcalase under high hydrostatic pressure. *Innovative Food Science & Emerging Technologies*, 43, 92-101. <http://dx.doi.org/10.1016/j.ifset.2017.08.001>.
- Zhang, T., Lv, C., Yun, S., Liao, X., Zhao, G., & Leng, X. (2012). Effect of high hydrostatic pressure (HHP) on structure and activity of phytoferritin. *Food Chemistry*, 130(2), 273-278. <http://dx.doi.org/10.1016/j.foodchem.2011.07.034>.
- Zhao, F., Liu, X. M., Ding, X. Z., Dong, H. Z., & Wang, W. T. (2019). Effects of high-intensity ultrasound pretreatment on structure, properties, and enzymolysis of soy protein isolate. *Molecules*, 24(20), 3637-3653. <http://dx.doi.org/10.3390/molecules24203637>. PMid:31600956.
- Zhao, F., Zhang, D., Li, X., & Dong, H. (2018). High-pressure homogenization pretreatment before enzymolysis of soy protein isolate: the effect of pressure level on aggregation and structural conformations of the protein. *Molecules*, 23(7), 1775-1788. <http://dx.doi.org/10.3390/molecules23071775>. PMid:30029493.
- Zhu, Z., Zhu, W., Yi, J., Liu, N., Cao, Y., Lu, J., Decker, E. A., & McClements, D. J. (2018). Effects of sonication on the physicochemical and functional properties of walnut protein isolate. *Food Research International*, 106, 853-861. <http://dx.doi.org/10.1016/j.foodres.2018.01.060>. PMid:29579996.